

Thermodynamic Geometry of Black Holes Enclosed by a Cavity in Extended Phase Space

Peng Wang^{*} and Feiyu Yao[†]

Center for Theoretical Physics, College of Physics, Sichuan University, Chengdu, 610064, China

Recently, the phase space of black holes in a spherical cavity of radius r_B has been extended by introducing a thermodynamic volume $V \equiv 4\pi r_B^3/3$. In the extended phase space, we consider the thermodynamic geometry, which provides a powerful tool to understand the microscopic structure of black holes, of Reissner-Nordström (RN) black holes in a cavity, as well as that of Reissner-Nordström-AdS black holes. Although the phase structures of the cavity and AdS cases show striking resemblance, we find that there exist significant differences between the thermodynamic geometries of these two cases. In particular, a reentrant transition of the type of the microstructure interactions, i.e., repulsive \rightarrow attractive \rightarrow repulsive with increasing temperature in an isobaric process, is observed for RN black holes in a cavity.

CONTENTS

I. Introduction	1
II. RN-AdS Black Holes	2
III. RN Black Holes in a Cavity	6
IV. Discussions and Conclusions	10
Acknowledgments	11
References	11

I. INTRODUCTION

Black hole thermodynamics has been of crucial importance in our understanding of quantum gravity. Since classical black holes absorb all matter and emit nothing, black holes were not considered to be thermodynamic systems until the Hawking's area theorem was proposed [1]. Bekenstein subsequently noticed a possible relation between the area theorem and the second law of thermodynamics [2]. The discovery of the Hawking radiation then assigns black holes a temperature [3, 4], which further confirms the analogy between usual thermodynamics and black hole mechanics. Consequently, the “four laws of black hole mechanics” were proposed and formulated by Bardeen, Carter, and Hawking [5]. Since the advent of the AdS/CFT correspondence [6–8], of particular interest are asymptotically anti-de Sitter (AdS) black holes, which can be thermodynamically stable as AdS boundary plays a role of a reflecting wall. Moreover, the first law becomes consistent with the corresponding Smarr relation, and black hole mass is interpreted as a chemical enthalpy [9]. After the Hawking-Page phase transition was observed in Schwarzschild-AdS black holes [10], thermodynamic properties and phase behavior of various more complicated black holes have been studied [11–35].

On the other hand, York first reported that a Schwarzschild black hole enclosed by a cavity can be thermally stable and also experiences a Hawking-Page-like transition to the thermal flat space as the temperature decreases [36]. Later, thermodynamics of Reissner-Nordström (RN) black holes in a cavity was discussed in a grand canonical ensemble [37] and a canonical ensemble [38, 39]. Like RN-AdS black holes, it showed that a Hawking-Page-like phase transition occurs in the grand canonical ensemble, and a van der Waals-like phase transition occurs in the canonical ensemble. Moreover, Hawking-Page-like or van der Waals-like phase transitions have also been found in the brane systems [40–45]. Properties of boson stars and hairy black holes in a cavity were also investigated [46–51], which were shown to closely resemble those of holographic superconductors in the AdS gravity. Later, the authors

^{*} pengw@scu.edu.cn

[†] yaofeiyu@stu.scu.edu.cn

of [52] studied the phase structure and transitions of Gauss-Bonnet black holes in a cavity, which are quite similar to the AdS counterparts. However, it has been reported that black holes in a cavity and the AdS counterparts can show different thermodynamic behavior, e.g., phase structure of Born-Infeld black holes [53, 54], the second law of thermodynamics [55] and thermodynamic geometry of RN black holes [56]. Furthermore, thermodynamics and critical behavior of de Sitter black holes in a cavity were investigated in [57–59]. To make the thermodynamics of black holes in a cavity become more complete, we recently extended the phase space of black holes in a cavity by including a thermodynamic pressure and a thermodynamic volume [60]. It showed that, in these extended phase spaces, the thermodynamic behavior of black holes in a cavity closely resembles that of the AdS counterparts, both exhibiting well-known phenomena found in previous studies, such as Hawking-Page-like and van der Waals-like phase transitions.

Although the idea that black hole can be understood as a thermodynamic system has convinced most people, the statistical description of the black hole microstates has not yet been fully understood, which has a deep impact upon the understanding of quantum gravity. On the other hand, the thermodynamic geometry method provides a useful tool to probe into microstructure of black holes. Inspired by the pioneering work of Weinhold [61], Ruppeiner [62] introduced a Riemannian thermodynamic entropy metric to describe the thermodynamic fluctuation theory and proposed a systematic way to calculate the Ricci curvature scalar R of the Ruppeiner metric. It showed that the sign of R can relate to the type of interparticle interactions: $R > 0$ corresponds to a repulsive interaction (e.g., ideal Bose gas), $R < 0$ to an attractive interaction (e.g., ideal Fermi gas), and $R = 0$ to no interaction (e.g., ideal gas). At a critical point, $|R|$ diverges as the correlation volume. Since the work of [63], thermodynamic geometry has been explored for various black holes [64–74]. Interestingly, RN-AdS black holes have been proposed to be built of some micromolecules, interactions among which can be tested by R [27, 33]. For a RN-AdS black hole in the extended phase space, it was observed that R can be positive or negative, and the critical behavior resembles that of ordinary thermodynamic systems [75–79]. Subsequently, thermodynamic geometry was investigated for other AdS black holes in the extended phase space [80–92].

Nevertheless, thermodynamic geometry has rarely been reported for black holes in cavity in the context of the extended phase space. In this paper, we investigate the thermodynamic geometry of RN black holes in cavity in the extended phase space. The rest of this paper is organized as follows. In section II, we discuss the phase structure and the thermodynamic geometry of RN-AdS black holes in the extended phase space. In section III, the phase structure and the thermodynamic geometry of RN black hole in a cavity are studied in the extended phase space. We summarize our results with a brief discussion in section IV. For simplicity, we set $G = \hbar = c = k_B = 1$ in this paper.

II. RN-ADS BLACK HOLES

In this section, we study the phase structure and the thermodynamic geometry of RN-AdS black holes in the extended phase space. The thermodynamic geometry, also known as the Ruppeiner geometry, is an important concept in understanding the microstructure of a thermodynamic system from its macroscopic quantities. Adopting the Ruppeiner approach, one can define the Ruppeiner metric $g_{\mu\nu}^R$ for a thermodynamic system of independent variables x^μ as

$$g_{\mu\nu}^R = -\frac{\partial^2 S(x)}{\partial x^\mu \partial x^\nu}, \quad (1)$$

where S is the entropy of the system. Then one can define a scalar curvature, namely the Ruppeiner invariant R , in this parameter space with the Ruppeiner metric (1). Note that $R > 0$ ($R < 0$) implies a repulsive (attractive) interaction. In this paper, we study the Ruppeiner geometry with the internal energy and the volume being fluctuation variables, corresponding to $x^\mu = (U, V)$. Therefore, the Ruppeiner metric becomes [88]

$$g_{\mu\nu}^R dx^\mu dx^\nu = d\left(\frac{1}{T}\right) dU + d\left(\frac{P}{T}\right) dV = \frac{1}{T} dT dS - \frac{1}{T} dV dP. \quad (2)$$

The 4-dimensional static charged RN-AdS black hole solution is described by

$$ds^2 = -f(r) dt^2 + \frac{dr^2}{f(r)} + r^2 (d\theta^2 + \sin^2 \theta d\phi^2), \quad A = -\frac{Q}{r} dt, \quad (3)$$

where the metric function $f(r)$ is

$$f(r) = 1 - \frac{2M}{r} + \frac{Q^2}{r^2} + \frac{r^2}{l^2}, \quad (4)$$

and l is the AdS radius. Here, the parameters M and Q are the black hole mass and charge, respectively. The Hawking temperature T is given by

$$T = \frac{1}{4\pi r_+} \left(1 + \frac{3r_+^2}{l^2} - \frac{Q^2}{r_+^2} \right), \quad (5)$$

where r_+ is the radius of the event horizon, satisfying $f(r_+) = 0$. The mass M can also be expressed in terms of r_+ ,

$$M = \frac{r_+}{2} \left(1 + \frac{Q^2}{r_+^2} + \frac{r_+^2}{l^2} \right). \quad (6)$$

Defining the pressure [93],

$$P \equiv \frac{3}{8\pi l^2}, \quad (7)$$

one can have

$$T = \frac{1}{4\pi r_+} \left(1 + 8\pi r_+^2 P - \frac{Q^2}{r_+^2} \right), \quad M = \frac{r_+}{2} \left(1 + \frac{Q^2}{r_+^2} + \frac{8}{3}\pi r_+^2 P \right). \quad (8)$$

Moreover, the entropy obeys the Bekenstein-Hawking area entropy relation,

$$S = \frac{A}{4} = \pi r_+^2, \quad (9)$$

and the thermodynamic volume is given by

$$V \equiv \frac{\partial M}{\partial P} = \frac{4}{3}\pi r_+^3. \quad (10)$$

For later convenience, we rescale thermodynamic variables,

$$\tilde{r}_+ \equiv r_+/Q, \quad \tilde{T} \equiv TQ, \quad \tilde{P} \equiv PQ^2, \quad \tilde{V} \equiv V/Q^3, \quad \tilde{G} \equiv G/Q, \quad (11)$$

where $G = M - TS$ is the Gibbs free energy, and tilde quantities are dimensionless. The rescaled thermodynamic variables can be expressed as

$$\tilde{V}(\tilde{r}_+) = \frac{4}{3}\pi\tilde{r}_+^3, \quad \tilde{T}(\tilde{r}_+, \tilde{P}) = \frac{1}{4\pi\tilde{r}_+} \left(1 + 8\pi\tilde{r}_+^2\tilde{P} - \frac{1}{\tilde{r}_+^2} \right), \quad \tilde{G}(\tilde{r}_+, \tilde{P}) = \frac{1}{12\tilde{r}_+} \left(9 + 3\tilde{r}_+^2 - 8\pi\tilde{r}_+^4\tilde{P} \right). \quad (12)$$

For the convenience of calculation, one can rewrite the Ruppeiner metric (2) in the (T, V) coordinate [88],

$$g_{\mu\nu}^R dx^\mu dx^\nu = \frac{1}{T^2} \left[C_V dT^2 - T \left(\frac{\partial P}{\partial V} \right)_T dV^2 \right]. \quad (13)$$

However, $C_V = T \left(\frac{\partial S}{\partial T} \right)_V = 0$ for a RN-AdS black hole, which gives that the metric is not invertible, and the Ruppeiner invariant R diverges. Compared with the specific heat capacity of the Van der Waals (VdW) fluid, $C_V^{VdW} = 3k_B/2$, the specific heat capacity of the RN-AdS black hole can be treated as the limit of the VdW fluid with $k_B \rightarrow 0$. Then one can regularize the divergent Ruppeiner invariant by normalizing it with C_V [88]. In other words, one can treat C_V as a constant whose value is infinitesimally close to zero and define a normalized Ruppeiner invariant,

$$\bar{R}(\tilde{r}_+, \tilde{P}) \equiv RC_V = \frac{2(\tilde{r}_+^2 - 2)(8\pi\tilde{r}_+^4\tilde{P} + 1)}{(\tilde{r}_+^2 - 3 - 8\pi\tilde{r}_+^4\tilde{P})^2}. \quad (14)$$

In FIG. 1, we present the region-plot of \bar{R} in the \tilde{P} - \tilde{r}_+ plane, where $\bar{R} < 0$ ($\bar{R} > 0$) in the red (blue) region, and $\bar{R} \rightarrow +\infty$ on the red line. The critical point, denoted by a black dot, lies on the $\bar{R} = +\infty$ line. Note that black hole solutions do not exist in the gray region, where T is negative. And the interaction is attractive for small enough horizon radius, while the interaction is repulsive for large enough horizon radius.

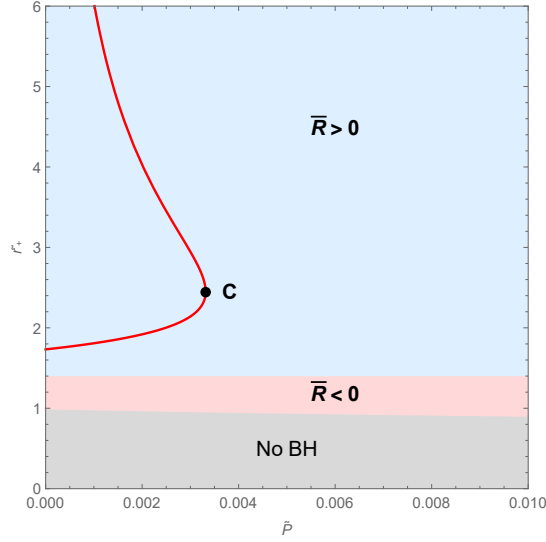


FIG. 1. The region-plot of the Ruppeiner invariant for RN-AdS black holes in the \tilde{P} - \tilde{r}_+ plane, where \tilde{r}_+ is the rescaled event horizon radius and \tilde{P} is the rescaled pressure. In the red (blue) region, $\bar{R} < 0$ ($\bar{R} > 0$). The red line corresponds to $\bar{R} = +\infty$. The black dot C denotes the critical point, which lies on the $\bar{R} = +\infty$ line. Black hole solutions do not exist in the gray region.

To study phase structure, we consider the Gibbs free energy

$$\tilde{G}(\tilde{r}_+, \tilde{P}) = \frac{1}{12\tilde{r}_+} \left(9 + 3\tilde{r}_+^2 - 8\tilde{P}\pi\tilde{r}_+^4 \right). \quad (15)$$

Solving eqn. (12) for \tilde{r}_+ in terms of \tilde{T} gives $\tilde{r}_+ = \tilde{r}_+(\tilde{T}, \tilde{P})$. It shows that $\tilde{r}_+(\tilde{T}, \tilde{P})$ is multi-valued for small enough \tilde{P} and single-valued for large enough \tilde{P} , which indicates that there is a critical point. The critical point is determined by

$$\frac{\partial \tilde{T}(\tilde{r}_+, \tilde{P})}{\partial \tilde{r}_+} = 0, \quad \frac{\partial^2 \tilde{T}(\tilde{r}_+, \tilde{P})}{\partial \tilde{r}_+^2} = 0, \quad (16)$$

which gives the critical values,

$$\tilde{r}_{+c} = \sqrt{6}, \quad \tilde{P}_c = \frac{1}{96\pi}, \quad \tilde{T}_c = \frac{1}{3\sqrt{6}\pi}. \quad (17)$$

If $\tilde{r}_+(\tilde{T}, \tilde{P})$ is multi-valued, there is more than one black hole solution for fixed values of \tilde{P} and \tilde{T} , corresponding to multiple phases in a canonical ensemble. Plugging $\tilde{r}_+(\tilde{T}, \tilde{P})$ into eqns. (14) and (15), one can have $\tilde{G}(\tilde{T}, \tilde{P})$ and $\bar{R}(\tilde{T}, \tilde{P})$.

When $\tilde{P} < \tilde{P}_c$, there are three solutions coexisting for some range of \tilde{T} . In fact, we plot \tilde{G} and \bar{R} against \tilde{T} in FIG. 2, which shows that three solutions, dubbed Large BH, Small BH and Intermediate BH, coexist for $\tilde{T}_1 < \tilde{T} < \tilde{T}_2$. Intermediate BH is a thermally unstable phase, while Small and Large BHs are thermally stable. The upper row of FIG. 2 shows that there is a first-order phase transition between Small BH and Large BH at $\tilde{T} = \tilde{T}_p$ with $\tilde{T}_1 < \tilde{T}_p < \tilde{T}_2$. The bottom row displays that \bar{R} of Large BH and Intermediate BH are always positive, corresponding to repulsive interactions between BH molecules. For Large BH and Small BH, $\bar{R} \rightarrow \infty$ at $\tilde{T} = \tilde{T}_1$ and $\tilde{T} = \tilde{T}_2$, respectively. Moreover, for Small BH, $\bar{R} = -1/2$ for $\tilde{T} = 0$, and $\bar{R} \rightarrow \infty$ for $\tilde{T} = \tilde{T}_2$, indicating that there exists $\bar{R} = 0$ at $\tilde{T} = \tilde{T}_{R_0}$. Furthermore, we find that $\tilde{T}_{R_0} < \tilde{T}_p$ when $\tilde{P} > \tilde{P}_I = 3/[32(9 + 4\sqrt{5})\pi]$, and $\tilde{T}_{R_0} > \tilde{T}_p$ when $\tilde{P} < \tilde{P}_I$. The case with $\tilde{P} = 0.001 < \tilde{P}_I$ is shown in the left column of FIG. 2, which displays that the phase transition occurs before $\tilde{T} = \tilde{T}_{R_0}$ as \tilde{T} increases from 0. Since \bar{R} is always positive for Large BH, the attractive interactions between the BH molecules turns into the repulsive one when the phase transition occurs. For $\tilde{P}_I < \tilde{P} < \tilde{P}_c$, the right column of FIG. 2 shows that as one increases \tilde{T} from 0, the attractive interaction turns into the repulsive one before the phase transition occurs.

When $\tilde{P} > \tilde{P}_c$, there is a single thermally stable solution for a fixed \tilde{T} . We plot \tilde{G} and \bar{R} against \tilde{T} for $\tilde{P} = 0.004$ in FIG. 3. The right panel of FIG. 3 displays that $\bar{R} = 0$ at $\tilde{T} = \tilde{T}_{R_0}$, and \bar{R} has a maximum at $\tilde{T} = \tilde{T}_{R_M}$. As one

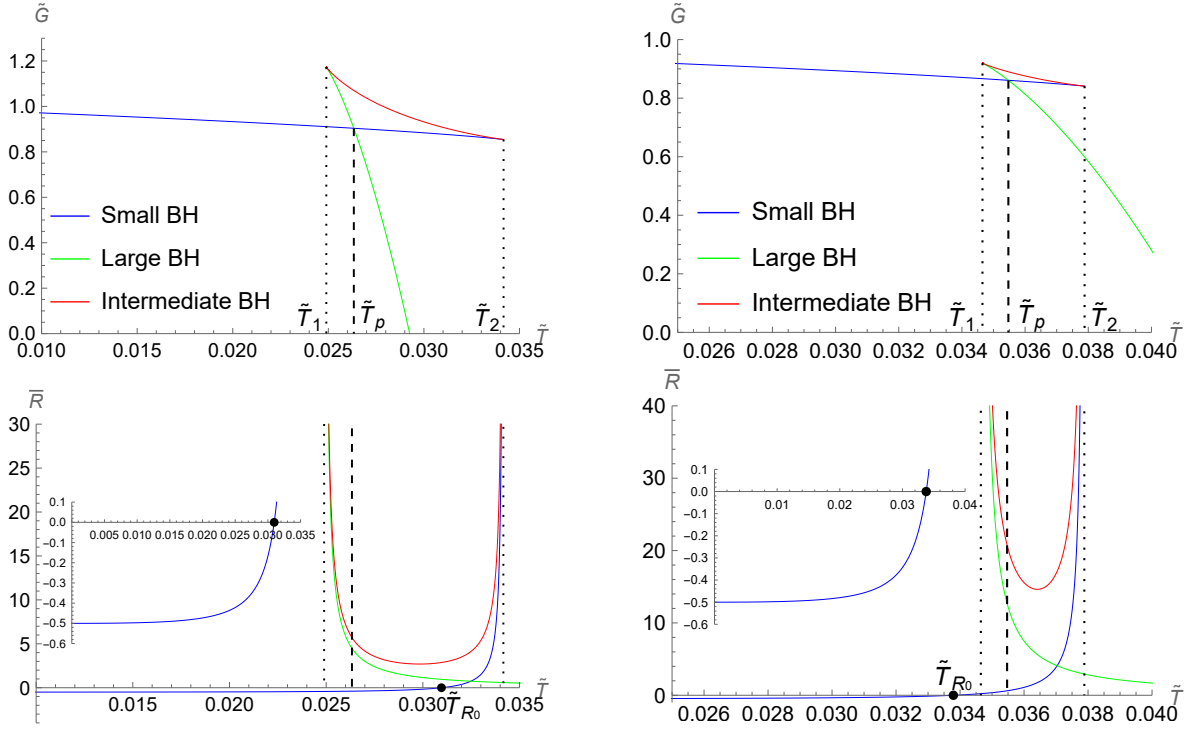


FIG. 2. Plots of the rescaled Gibbs free energy \tilde{G} and the normalized Ruppeiner invariant \bar{R} against the rescaled temperature \tilde{T} for RN-AdS black holes when $\tilde{P} < \tilde{P}_c$. There are three black hole solutions when $\tilde{T}_1 < \tilde{T} < \tilde{T}_2$. As \tilde{T} increases from 0, a first-order transition from Small BH to Large BH occurs at $\tilde{T} = \tilde{T}_p$. The black points correspond to $\bar{R} = 0$ at $\tilde{T} = \tilde{T}_{R_0}$. **Left Column:** $\tilde{P} = 0.001$, one has $\tilde{T}_{R_0} > \tilde{T}_p$. As one increases \tilde{T} from 0, the attractive interaction turns repulsive when the phase transition occurs, and \bar{R} cannot be 0 for the thermodynamically preferred phase. **Right Column:** $\tilde{P} = 0.002$, one has $\tilde{T}_{R_0} < \tilde{T}_p$. As one increases \tilde{T} from 0, the attractive interaction turns repulsive before the phase transition occurs.

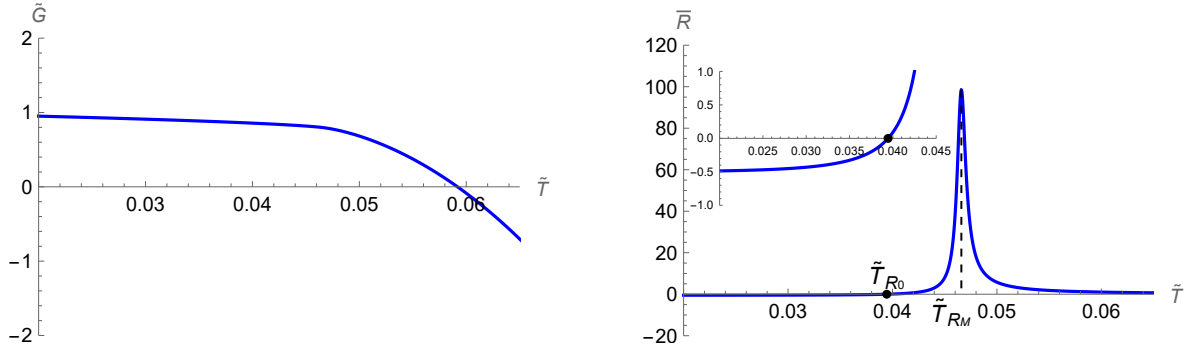


FIG. 3. Plots of the rescaled Gibbs free energy \tilde{G} and the normalized Ruppeiner invariant \bar{R} against the rescaled temperature \tilde{T} for RN-AdS black holes with $\tilde{P} = 0.004 > \tilde{P}_c$. There is only one branch and no phase transition. The normalized Ruppeiner invariant $\bar{R} = -1/2$ when $\tilde{T} = 0$, and $\bar{R} \rightarrow 0$ when $\tilde{T} \rightarrow \infty$. The black point corresponds to $\bar{R} = 0$. And \bar{R} has a maximum at $\tilde{T} = \tilde{T}_{RM}$.

increases \tilde{T} from 0, \bar{R} becomes 0 at $\tilde{T} = \tilde{T}_{R_0} < \tilde{T}_{RM}$, and \bar{R} is always positive for $\tilde{T} > \tilde{T}_{R_0}$, which means that the attractive interaction turns repulsive at $\tilde{T} = \tilde{T}_{R_0}$.

In FIG. 4, we display the globally preferred phases of RN-AdS black holes, and the regions of $\bar{R} > 0$ and $\bar{R} < 0$ in the \tilde{P} - \tilde{T} plane. The black line is the first-order phase transition line, separating Large BH and Small BH. And it terminates at a critical point, marked by a black dot. In the blue (red) region, one has $\bar{R} > 0$ ($\bar{R} < 0$), which means that the type of interactions between BH molecules is repulsive (attractive). Note that \bar{R} is always finite in the \tilde{P} - \tilde{T}

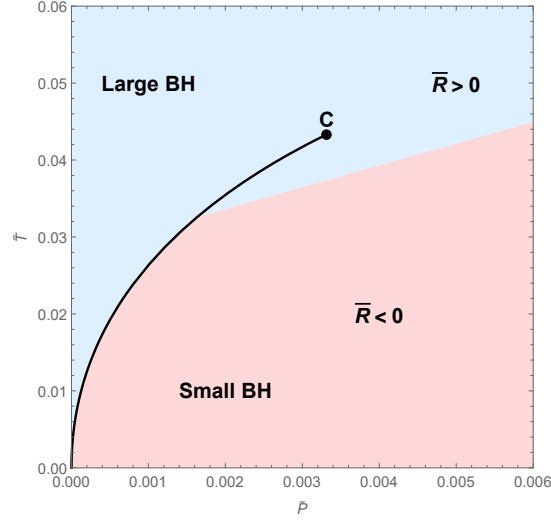


FIG. 4. Phase diagram of RN-AdS black holes in the \tilde{P} - \tilde{T} plane. The first-order phase transition line, separating Large BH and Small BH, is displayed by a black line and terminates at the critical point, marked by a black dot. The blue region and red region correspond to repulsive and attractive interactions, respectively.

plane.

III. RN BLACK HOLES IN A CAVITY

In this section, we study the phase structure and the thermodynamic geometry of RN black holes enclosed by a spherical cavity in an extended phase space. The 4-dimensional RN black hole solution is

$$ds^2 = -f(r) dt^2 + \frac{dr^2}{f(r)} + r^2 (d\theta^2 + \sin^2 \theta d\phi^2), \quad (18)$$

where the metric function is

$$f(r) = \left(1 - \frac{r_+}{r}\right) \left(1 - \frac{Q_b^2}{r_+ r}\right), \quad (19)$$

and the electromagnetic potential is

$$A = -\frac{Q_b}{r} dt. \quad (20)$$

Here, Q_b is the black hole charge, and r_+ is the radius of the event horizon. The Hawking temperature T_b of the RN black hole is given by

$$T_b = \frac{1}{4\pi r_+} \left(1 - \frac{Q_b^2}{r_+^2}\right). \quad (21)$$

The wall of the cavity, which is located at $r = r_B$, is maintained at a temperature of T and a charge of Q . It can show that the system temperature T and charge Q can be related to the black hole temperature T_b and charge Q_b as [37]

$$Q = Q_b \text{ and } T = \frac{T_b}{\sqrt{f(r_B)}}, \quad (22)$$

respectively. Moreover, the Helmholtz free energy F and the thermal energy E were also given in [38],

$$F = r_B \left[1 - \sqrt{f(r_B)}\right] - \pi T r_+^2, \quad E = r_B \left[1 - \sqrt{f(r_B)}\right]. \quad (23)$$

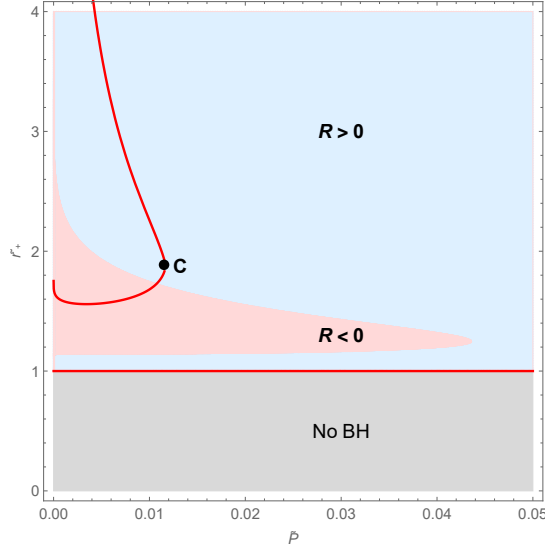


FIG. 5. The region-plot of the Ruppeiner invariant R for RN black holes in a cavity in the \tilde{P} - \tilde{r}_+ plane, where \tilde{r}_+ is the rescaled event horizon radius, and \tilde{P} is the rescaled pressure. In the red (blue) region, one has $R < 0$ ($R > 0$). The red line in the red region correspond to $R \rightarrow -\infty$, and that in the blue region to $R \rightarrow +\infty$. The critical point is marked by C and lies on the $R \rightarrow +\infty$ line. Black hole solutions do not exist in the gray region since RN black holes in a cavity have a minimum temperature for a given \tilde{P} .

In [60], we introduced a thermodynamic volume,

$$V \equiv 4\pi r_B^3/3, \quad (24)$$

and the conjugate thermodynamic pressure,

$$P = -\partial E/\partial V, \quad (25)$$

as a pair of extra thermodynamic variables for black holes in a cavity. In this extended phase space, the Gibbs free energy, $G = F + PV$, is considered for a constant pressure system. Similar to the AdS case, we also consider the Ruppeiner metric (2) and use eqns. (22) and (24) to calculate the Ruppeiner invariant R . Unlike the RN-AdS black holes, we find that the Ruppeiner invariant R of RN black holes in a cavity does not need any regularization.

Defining rescaled thermodynamic variables,

$$\tilde{r}_+ \equiv r_+/Q, \tilde{r}_B \equiv r_B/Q, \tilde{T} \equiv TQ, \tilde{P} \equiv PQ^2, \tilde{V} \equiv V/Q^3, \tilde{G} \equiv G/Q, \tilde{R} = RQ^2, \quad (26)$$

we obtain

$$\begin{aligned} \tilde{T}(\tilde{r}_+, \tilde{r}_B) &= \frac{1}{4\pi\tilde{r}_+} \left(1 - \frac{1}{\tilde{r}_+^2}\right) \sqrt{\frac{\tilde{r}_B^2\tilde{r}_+}{(\tilde{r}_B - \tilde{r}_+)(\tilde{r}_+\tilde{r}_B - 1)}}, \\ \tilde{P}(\tilde{r}_+, \tilde{r}_B) &= \frac{-1 + 2\tilde{r}_+\tilde{r}_B - \tilde{r}_+^2 - 2\sqrt{\tilde{r}_+(\tilde{r}_B - \tilde{r}_+)(\tilde{r}_+\tilde{r}_B - 1)}}{8\pi\tilde{r}_B^2\sqrt{\tilde{r}_+(\tilde{r}_B - \tilde{r}_+)(\tilde{r}_+\tilde{r}_B - 1)}}. \end{aligned} \quad (27)$$

Solving $\tilde{P}(\tilde{r}_+, \tilde{r}_B) = \tilde{P}$ for \tilde{r}_B in terms of \tilde{r}_+ and \tilde{P} gives $\tilde{r}_B = \tilde{r}_B(\tilde{r}_+, \tilde{P})$, via which we can express the rescaled Ruppeiner invariant \tilde{R} as a function of \tilde{r}_+ and \tilde{P} . In FIG. 5, we display the region-plot of \tilde{R} in the \tilde{P} - \tilde{r}_+ plane. In the red and blue regions, one has $\tilde{R} < 0$ and $\tilde{R} > 0$, respectively. Moreover, $\tilde{R} = \pm\infty$ corresponds to the red lines. Note that $\tilde{R} = +\infty$ at the critical point which is marked by a black point and determined by

$$\frac{\partial \tilde{T}(\tilde{r}_+, \tilde{P})}{\partial \tilde{r}_+} = 0, \quad \frac{\partial^2 \tilde{T}(\tilde{r}_+, \tilde{P})}{\partial \tilde{r}_+^2} = 0. \quad (28)$$

The associated critical values are obtained by solving the above equations

$$\tilde{r}_{+c} = 1.888, \tilde{P}_c = 0.0115, \tilde{T}_c = 0.118. \quad (29)$$

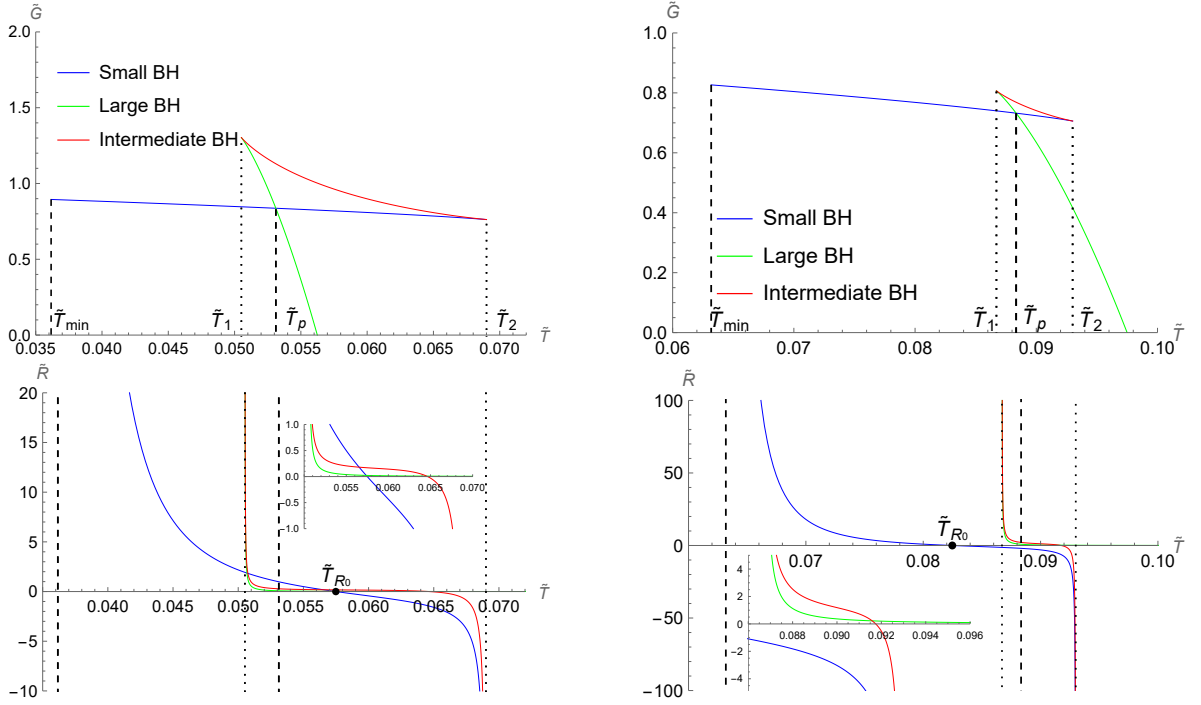


FIG. 6. Plots of the rescaled Gibbs free energy \tilde{G} and the rescaled Ruppeiner invariant \tilde{R} against the rescaled temperature \tilde{T} for RN black holes in a cavity with the rescaled pressure $\tilde{P} = 0.002$ (left column) and 0.006 (right column). There are three black hole phases for $\tilde{T}_1 < \tilde{T}_p < \tilde{T}_2$, and a first-order transition between Small BH and Large BH occurring at $\tilde{T} = \tilde{T}_p$. For Small and Intermediate BHs, $\tilde{R} = -\infty$ at $\tilde{T} = \tilde{T}_2$. The black points correspond to $\tilde{R} = 0$ at $\tilde{T} = \tilde{T}_{R_0}$. **Left Column:** $\tilde{T}_{R_0} > \tilde{T}_p$. The interactions of the globally preferred phases are always repulsive. **Right Column:** $\tilde{T}_{R_0} < \tilde{T}_p$. For the globally preferred phases, the type of interactions changes from repulsive to attractive at $\tilde{T} = \tilde{T}_{R_0}$ and then returns to repulsive at $\tilde{T} = \tilde{T}_p$ as \tilde{T} increases from \tilde{T}_{\min} .

Black hole solutions do not exist in the gray region since a RN black hole in a cavity has a minimum of temperature T_{\min} for a nonzero \tilde{P} [60]. Unlike RN-AdS black holes, the Ruppeiner invariant R of RN black holes in a cavity can be negative infinity in some parametric region.

Furthermore, we can obtain \tilde{r}_+ as a function of \tilde{T} and \tilde{P} by solving eqn. (27), and then express \tilde{G} and \tilde{R} in terms of \tilde{T} and \tilde{P} . With $\tilde{G}(\tilde{T}, \tilde{P})$ and $\tilde{R}(\tilde{T}, \tilde{P})$, we can discuss the phase structure of RN black holes in a cavity for given \tilde{T} and \tilde{P} , and compute the Ruppeiner invariant of each phase. In the extended phase spaces, it has been shown that the phase structure of RN black holes in a cavity is similar to that of AdS counterparts [60]. Specifically, FIGs. 6 and 7 show that, when $\tilde{P} < \tilde{P}_c$, RN black holes in a cavity have three phases, namely Small BH, Intermediate BH and Large BH, coexisting for $\tilde{T}_1 < \tilde{T} < \tilde{T}_2$, and there is a first-order phase transition between Small BH and Large BH occurring at $\tilde{T} = \tilde{T}_p$. However, the behavior of the Ruppeiner invariant is quite richer than the AdS case. In fact, we find

- $\tilde{P} < \tilde{P}_1 \simeq 0.0108$. The \tilde{R} of Small BH decreases monotonically from positive infinity to negative infinity as one increases \tilde{T} from \tilde{T}_{\min} to \tilde{T}_2 . Therefore, there exists $\tilde{R} = 0$ at $\tilde{T} = \tilde{T}_{R_0}$, which could be greater or smaller than \tilde{T}_p . We present \tilde{G} and \tilde{R} as a function of \tilde{T} for $\tilde{P} = 0.002$ in the left column of FIG. 6, where $\tilde{T}_{R_0} > \tilde{T}_p$. Since \tilde{R} of Large BH is positive, \tilde{R} stays positive at the phase transition. So the globally preferred phases always have a positive \tilde{R} , corresponding to repulsive interactions. On the other hand, we consider the $\tilde{P} = 0.006$ case in the right column of FIG. 6, where $\tilde{T}_{R_0} < \tilde{T}_p$. Therefore, the globally preferred phases have a negative \tilde{R} when $\tilde{T}_{R_0} < \tilde{T} < \tilde{T}_p$, which means that, as one increase \tilde{T} from \tilde{T}_{\min} , the interactions are repulsive at first, then become attractive at $\tilde{T} = \tilde{T}_{R_0}$, and finally return to repulsive ones at $\tilde{T} = \tilde{T}_p$.
- $\tilde{P}_1 < \tilde{P} < \tilde{P}_c$. The \tilde{R} of Small BH is positively infinite at $\tilde{T} = \tilde{T}_2$ and \tilde{T}_{\min} , and has a negative minimum between \tilde{T}_2 and \tilde{T}_{\min} , which means $\tilde{R} = 0$ occurs at $\tilde{T} = \tilde{T}_{R_0S}$ and \tilde{T}_{R_0L} , respectively, with $\tilde{T}_{\min} < \tilde{T}_{R_0S} < \tilde{T}_{R_0L} < \tilde{T}_2$. Although we find \tilde{T}_{R_0S} is always smaller than \tilde{T}_p , \tilde{T}_{R_0L} may be smaller or greater than \tilde{T}_p . Note that Large BH always has a positive \tilde{R} . For $\tilde{P} = 0.0109$, \tilde{G} and \tilde{R} are plotted against \tilde{T} in the left column of FIG. 7, where

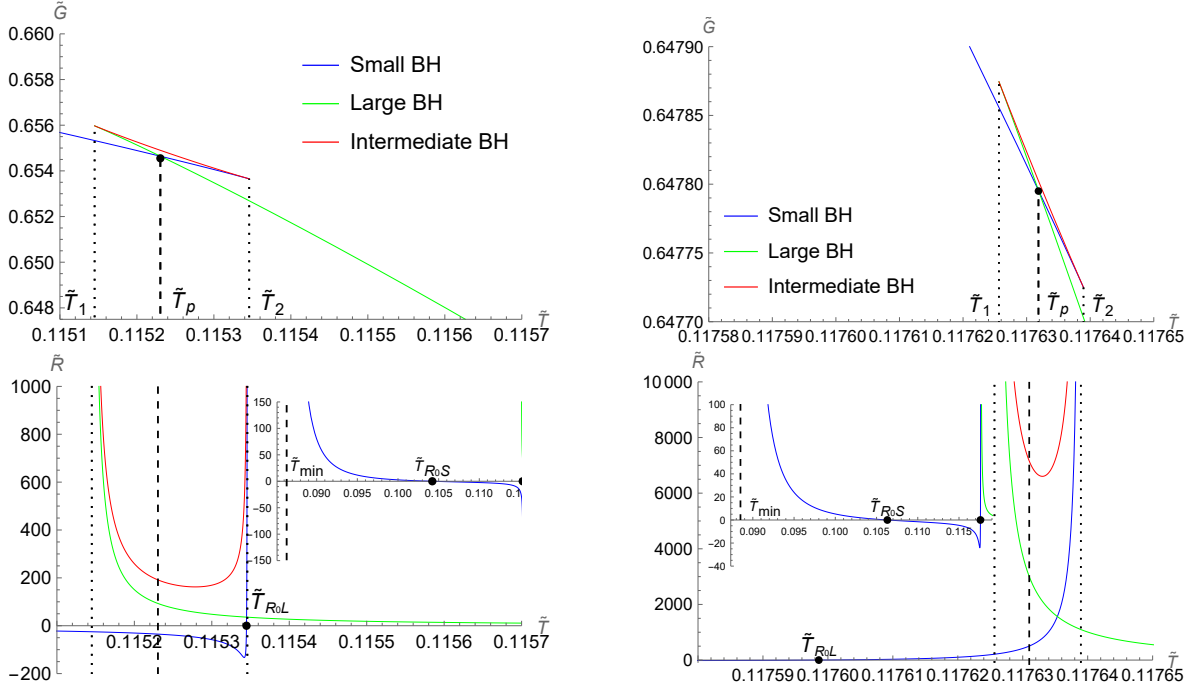


FIG. 7. Plots of the rescaled Gibbs free energy \tilde{G} and the rescaled Ruppeiner invariant \tilde{R} against the rescaled temperature \tilde{T} for RN black holes in a cavity with the rescaled pressure $\tilde{P} = 0.0109$ (left column) and 0.0114 (right column). Three black hole phases coexist for $\tilde{T}_1 < \tilde{T}_p < \tilde{T}_2$, during which a first-order transition between Small BH and Large BH occurs at $\tilde{T} = \tilde{T}_p$. The \tilde{R} of Large and Intermediate BHs are positive, whereas Small BH has a negative \tilde{R} for $\tilde{T}_{R_0S} < \tilde{T} < \tilde{T}_{R_0L}$ and vanishing \tilde{R} at $\tilde{T} = \tilde{T}_{R_0S}$ and \tilde{T}_{R_0L} , marked by black points. **Left Column:** $\tilde{T}_{R_0L} > \tilde{T}_p$. The microstructure interactions of the globally preferred phases turn attractive from repulsive at $\tilde{T} = \tilde{T}_{R_0S}$, and then return to repulsive at $\tilde{T} = \tilde{T}_p$ as one increases \tilde{T} from \tilde{T}_{\min} . **Right Column:** $\tilde{T}_p > \tilde{T}_{R_0L}$. For the globally preferred phases, the type of interactions changes from repulsive to attractive at $\tilde{T} = \tilde{T}_{R_0S}$ and then returns to repulsive at $\tilde{T} = \tilde{T}_{R_0L}$ as \tilde{T} increases from \tilde{T}_{\min} . However, the interactions remain repulsive during the phase transition at $\tilde{T} = \tilde{T}_p$.

$\tilde{T}_{R_0L} > \tilde{T}_p$. In this case, the globally preferred phases have a negative \tilde{R} and hence attractive interactions for $\tilde{T}_{R_0S} < \tilde{T} < \tilde{T}_p$. When $\tilde{T} > \tilde{T}_p$ or $\tilde{T} < \tilde{T}_{R_0S}$, the interactions of the globally preferred phases are repulsive, which indicates that the type of the interactions changes during the phase transition. We show the $\tilde{P} = 0.0114$ case in the right column of FIG. 7, where $\tilde{T}_{R_0L} < \tilde{T}_p$. At $\tilde{T} = \tilde{T}_p$, Large and Small BHs both have a positive \tilde{R} , indicating that the type of the interactions remains repulsive during the phase transition. Moreover, as \tilde{T} increases from \tilde{T}_{\min} to \tilde{T}_p , the globally preferred phase (i.e., Small BH) undergoes repulsive microstructure interactions \rightarrow attractive ones \rightarrow repulsive ones.

When $\tilde{P} > \tilde{P}_c$, there is only one phase and no phase transition. We find that \tilde{R} always has a maximum and a minimum, and approaches positive infinity and zero as $\tilde{T} \rightarrow \tilde{T}_{\min}$ and $\tilde{T} \rightarrow \infty$, respectively. In the left column of FIG. 8, we plot \tilde{G} and \tilde{R} as a function of \tilde{T} for $\tilde{P} = 0.02$. In this case, \tilde{R} has two zeros at $\tilde{T} = \tilde{T}_{R_0S}$ and \tilde{T}_{R_0L} , and hence the microstructure interactions are attractive for $\tilde{T}_{R_0S} < \tilde{T} < \tilde{T}_{R_0L}$ and repulsive otherwise. The $\tilde{P} = 0.05$ case is plotted in the right column of FIG. 8, which shows that \tilde{R} is always positive, and therefore the microstructure interactions are always repulsive.

In FIG. 9, we present the globally preferred phases of RN black holes in a cavity in the \tilde{P} - \tilde{T} plane. The first-order phase transition between Large BH and Small BH is represented by a black line, and the second-order critical point is marked by a black dot. The phase diagram of RN black holes in a cavity is quite similar to that of RN-AdS black holes, except for the gray region where no black hole solutions exist. The region where $\tilde{R} > 0$ ($\tilde{R} < 0$) is displayed as the blue (red) region. It shows that the microstructure interactions are repulsive in most part of the parametric space, while the $\tilde{R} < 0$ region is an “island” in the \tilde{P} - \tilde{T} plane. The right panel of FIG. 9 highlights the region near the critical point, and exhibits that the interactions around the critical point are repulsive. Unlike RN-AdS black holes, the globally preferred phases of RN black holes in a cavity can have a divergent \tilde{R} on the red line, corresponding to black holes at $\tilde{T} = \tilde{T}_{\min}$.

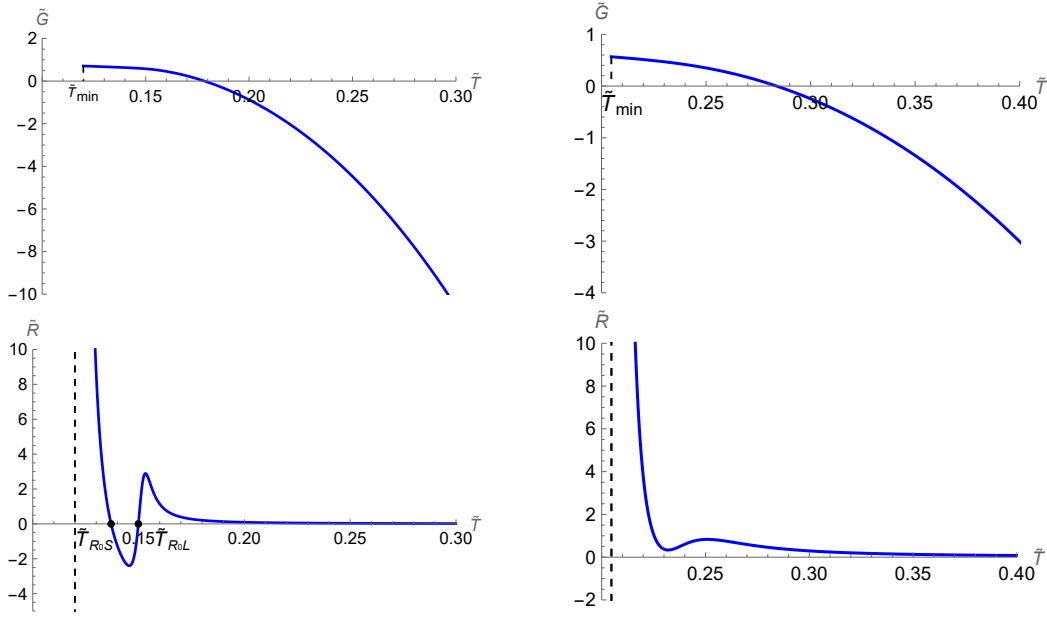


FIG. 8. Plots of the rescaled Gibbs free energy \tilde{G} and the rescaled Ruppeiner invariant \tilde{R} against the rescaled temperature \tilde{T} for RN black holes in a cavity when $\tilde{P} > \tilde{P}_c$. Since there is only one phase, no phase transitions occur. **Left Column:** $\tilde{P} = 0.02$. There are two zeros of $\tilde{R} = 0$, which are \tilde{T}_{R0S} and \tilde{T}_{R0L} , marked by black points. The interactions turn attractive from repulsive, and then return to repulsive as one increases \tilde{T} from \tilde{T}_{\min} . **Right Column:** $\tilde{P} = 0.05$. The microstructure interactions are always repulsive.

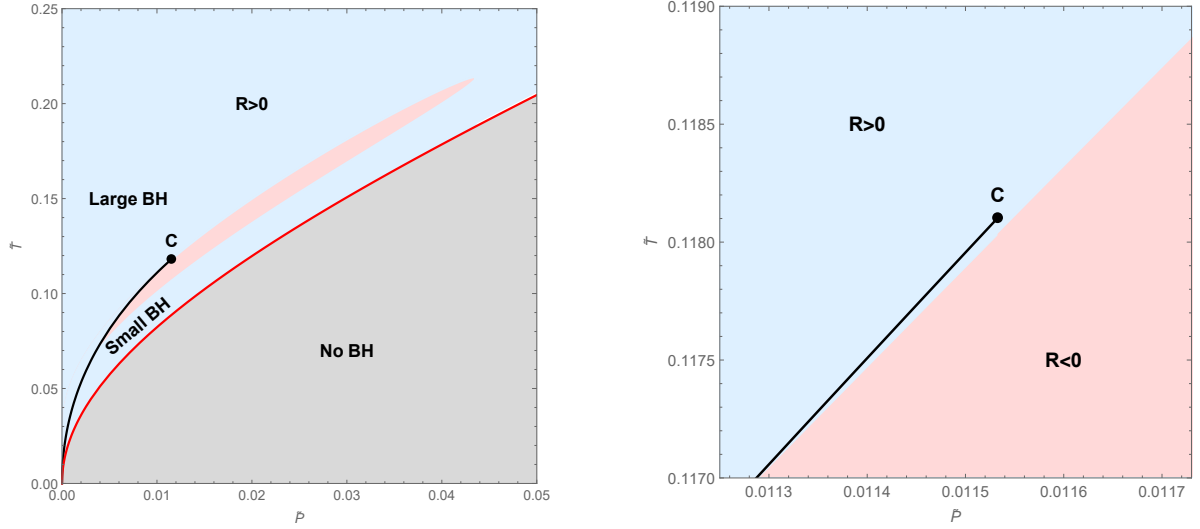


FIG. 9. Phase diagram of RN black holes in a cavity in the \tilde{P} - \tilde{T} plane. The black lines and black dots represent the first-order phase transition and the critical point, respectively. In the blue (red) region, $R > 0$ ($R < 0$), corresponding to repulsive (attractive) interactions. Black hole solutions do not exist in the gray region. On the red line, one has $R = +\infty$.

IV. DISCUSSIONS AND CONCLUSIONS

In this paper, we studied the phase structure and the thermodynamic geometry of charged (RN) black holes in the extended phase space by considering two kinds of boundary conditions, namely the asymptotically AdS boundary and the Dirichlet boundary in the asymptotically flat spacetime. For the extended phase space of RN-AdS black holes, the cosmological constant is interpreted as a pressure, and the conjugate thermodynamic volume then is $V =$

$4\pi r_+^3/3$ with r_+ being the horizon radius. In parallel with AdS black holes, we extended the phase space of RN black holes in a cavity by introducing a thermodynamic volume $V = 4\pi r_B^3/3$, where r_B is the radius of the cavity, and the conjugate pressure $P = -\partial E/\partial V$, where E is the thermal energy. In these extended phase spaces, we studied the thermodynamic geometry of charged black holes by taking the internal energy U and the volume V as fluctuation variables. Although the phase structures of the AdS and cavity cases were shown to be alike, we found that there are significant differences between the thermodynamic geometries in these two cases.

Specifically, we calculated the normalized Ruppeiner invariant $\bar{R} \equiv RC_V$ for RN-AdS black holes and the rescaled Ruppeiner invariant $\tilde{R} = RQ^2$ for RN black holes in a cavity. The behavior of \bar{R} and \tilde{R} as a function of the rescaled horizon radius \tilde{r}_+ and the rescaled pressure \tilde{P} were presented in FIGs. 1 and 5, respectively. In the AdS case, \bar{R} only diverges to positive infinity on the red line, and goes to $-1/2$ in the extremal limit. In the cavity case, \tilde{R} can diverge to negative infinity or positive infinity, and goes to positive infinity as the temperature approaches its minimum value. We displayed phase diagrams in the \tilde{T} - \tilde{P} plane of RN-AdS black holes and RN black holes in a cavity, as well as the parametric regions where $R > 0$ or $R < 0$, in FIGs. 4 and 9, respectively. For RN-AdS black holes with a fixed \tilde{P} , $\bar{R} = 0$ always has a single solution, corresponding to the change of the type of the microstructure interactions as \tilde{T} increases at a constant \tilde{P} . For RN black holes in a cavity with a given \tilde{P} , $\tilde{R} = 0$ has either no solution, indicating the interactions always stay repulsive as \tilde{T} increases at a constant \tilde{P} , or exactly two solutions, corresponding to a reentrant transition of the type of the interactions (i.e., repulsive \rightarrow attractive \rightarrow repulsive) as \tilde{T} increases at a constant \tilde{P} .

In existing studies, the thermodynamic geometry of RN black holes in a cavity was investigated in the normal phase space, in which the cavity radius is fixed [56]. It was found that the microstructure interactions always stay attractive before and after the LBH/SBH first-order transition. The behavior of the thermodynamic geometry has been shown to be richer in the extended phase space. On the other hand, black holes in a cavity have been observed to possess a lot of interesting thermodynamic behavior, e.g., the second law of thermodynamics and reentrant phase transitions, in the normal phase space [53–55]. It would be very inspiring to explore thermodynamic phenomena other than the thermodynamic geometry for black holes in a cavity in the extended phase space.

ACKNOWLEDGMENTS

We are grateful to Guangzhou Guo and Qingyu Gan for useful discussions and valuable comments. This work is supported in part by NSFC (Grant No. 11875196, 11375121, 11947225 and 11005016).

-
- [1] S.W. Hawking. Gravitational radiation from colliding black holes. *Phys. Rev. Lett.*, 26:1344–1346, 1971. [doi:10.1103/PhysRevLett.26.1344](#).
 - [2] Jacob D Bekenstein. Black holes and the second law. *Lett. Nuovo Cim.*, 4(15):737–740, 1972. [doi:10.1007/BF02757029](#).
 - [3] S.W. Hawking. Black hole explosions. *Nature*, 248:30–31, 1974. [doi:10.1038/248030a0](#).
 - [4] S.W. Hawking. Particle Creation by Black Holes. In *1st Oxford Conference on Quantum Gravity*, pages 219–267, 8 1975.
 - [5] James M. Bardeen, B. Carter, and S.W. Hawking. The Four laws of black hole mechanics. *Commun. Math. Phys.*, 31:161–170, 1973. [doi:10.1007/BF01645742](#).
 - [6] Juan Martin Maldacena. The Large N limit of superconformal field theories and supergravity. *Int. J. Theor. Phys.*, 38:1113–1133, 1999. [arXiv:hep-th/9711200](#), [doi:10.1023/A:1026654312961](#).
 - [7] S.S. Gubser, Igor R. Klebanov, and Alexander M. Polyakov. Gauge theory correlators from noncritical string theory. *Phys. Lett. B*, 428:105–114, 1998. [arXiv:hep-th/9802109](#), [doi:10.1016/S0370-2693\(98\)00377-3](#).
 - [8] Edward Witten. Anti-de Sitter space and holography. *Adv. Theor. Math. Phys.*, 2:253–291, 1998. [arXiv:hep-th/9802150](#), [doi:10.4310/ATMP.1998.v2.n2.a2](#).
 - [9] David Kastor, Sourya Ray, and Jennie Traschen. Entropy and the Mechanics of AdS Black Holes. *Class. Quant. Grav.*, 26:195011, 2009. [arXiv:0904.2765](#), [doi:10.1088/0264-9381/26/19/195011](#).
 - [10] S.W. Hawking and Don N. Page. Thermodynamics of Black Holes in anti-De Sitter Space. *Commun. Math. Phys.*, 87:577, 1983. [doi:10.1007/BF01208266](#).
 - [11] Edward Witten. Anti-de Sitter space, thermal phase transition, and confinement in gauge theories. *Adv. Theor. Math. Phys.*, 2:505–532, 1998. [arXiv:hep-th/9803131](#), [doi:10.4310/ATMP.1998.v2.n3.a3](#).
 - [12] Mirjam Cvetič and Steven S. Gubser. Phases of R charged black holes, spinning branes and strongly coupled gauge theories. *JHEP*, 04:024, 1999. [arXiv:hep-th/9902195](#), [doi:10.1088/1126-6708/1999/04/024](#).
 - [13] Andrew Chamblin, Roberto Emparan, Clifford V. Johnson, and Robert C. Myers. Charged AdS black holes and catastrophic holography. *Phys. Rev. D*, 60:064018, Aug 1999. URL: <https://link.aps.org/doi/10.1103/PhysRevD.60.064018>, [arXiv:hep-th/9902170](#), [doi:10.1103/PhysRevD.60.064018](#).
 - [14] Andrew Chamblin, Roberto Emparan, Clifford V. Johnson, and Robert C. Myers. Holography, thermodynamics and

- fluctuations of charged AdS black holes. *Phys. Rev. D*, 60:104026, Oct 1999. URL: <https://link.aps.org/doi/10.1103/PhysRevD.60.104026>, [arXiv:hep-th/9904197](https://arxiv.org/abs/hep-th/9904197), [doi:10.1103/PhysRevD.60.104026](https://doi.org/10.1103/PhysRevD.60.104026).
- [15] Marco M. Caldarelli, Guido Cognola, and Dietmar Klemm. Thermodynamics of Kerr-Newman-AdS black holes and conformal field theories. *Class. Quant. Grav.*, 17:399–420, 2000. [arXiv:hep-th/9908022](https://arxiv.org/abs/hep-th/9908022), [doi:10.1088/0264-9381/17/2/310](https://doi.org/10.1088/0264-9381/17/2/310).
- [16] Rong-Gen Cai. Gauss-Bonnet black holes in AdS spaces. *Phys. Rev. D*, 65:084014, 2002. [arXiv:hep-th/0109133](https://arxiv.org/abs/hep-th/0109133), [doi:10.1103/PhysRevD.65.084014](https://doi.org/10.1103/PhysRevD.65.084014).
- [17] Mirjam Cvetič, Shin’ichi Nojiri, and Sergei D. Odintsov. Black hole thermodynamics and negative entropy in de Sitter and anti-de Sitter Einstein-Gauss-Bonnet gravity. *Nucl. Phys. B*, 628:295–330, 2002. [arXiv:hep-th/0112045](https://arxiv.org/abs/hep-th/0112045), [doi:10.1016/S0550-3213\(02\)00075-5](https://doi.org/10.1016/S0550-3213(02)00075-5).
- [18] Shin’ichi Nojiri and Sergei D. Odintsov. Anti-de Sitter black hole thermodynamics in higher derivative gravity and new confining deconfining phases in dual CFT. *Phys. Lett. B*, 521:87–95, 2001. [Erratum: *Phys.Lett.B* 542, 301 (2002)]. [arXiv:hep-th/0109122](https://arxiv.org/abs/hep-th/0109122), [doi:10.1016/S0370-2693\(01\)01186-8](https://doi.org/10.1016/S0370-2693(01)01186-8).
- [19] Shao-Wen Wei and Yu-Xiao Liu. Critical phenomena and thermodynamic geometry of charged Gauss-Bonnet AdS black holes. *Phys. Rev. D*, 87(4):044014, Feb 2013. URL: <https://link.aps.org/doi/10.1103/PhysRevD.87.044014>, [arXiv:1209.1707](https://arxiv.org/abs/1209.1707), [doi:10.1103/PhysRevD.87.044014](https://doi.org/10.1103/PhysRevD.87.044014).
- [20] Sharmila Gunasekaran, Robert B. Mann, and David Kubiznak. Extended phase space thermodynamics for charged and rotating black holes and Born-Infeld vacuum polarization. *JHEP*, 11:110, 2012. [arXiv:1208.6251](https://arxiv.org/abs/1208.6251), [doi:10.1007/JHEP11\(2012\)110](https://doi.org/10.1007/JHEP11(2012)110).
- [21] Rong-Gen Cai, Li-Ming Cao, Li Li, and Run-Qiu Yang. P-V criticality in the extended phase space of Gauss-Bonnet black holes in AdS space. *JHEP*, 09:005, 2013. [arXiv:1306.6233](https://arxiv.org/abs/1306.6233), [doi:10.1007/JHEP09\(2013\)005](https://doi.org/10.1007/JHEP09(2013)005).
- [22] Wei Xu and Liu Zhao. Critical phenomena of static charged AdS black holes in conformal gravity. *Phys. Lett. B*, 736:214–220, 2014. [arXiv:1405.7665](https://arxiv.org/abs/1405.7665), [doi:10.1016/j.physletb.2014.07.019](https://doi.org/10.1016/j.physletb.2014.07.019).
- [23] Antonia M. Frassino, David Kubiznak, Robert B. Mann, and Fil Simovic. Multiple Reentrant Phase Transitions and Triple Points in Lovelock Thermodynamics. *JHEP*, 09:080, 2014. [arXiv:1406.7015](https://arxiv.org/abs/1406.7015), [doi:10.1007/JHEP09\(2014\)080](https://doi.org/10.1007/JHEP09(2014)080).
- [24] M. H. Dehghani, S. Kamrani, and A. Sheykhi. $P-V$ criticality of charged dilatonic black holes. *Phys. Rev. D*, 90(10):104020, 2014. [arXiv:1505.02386](https://arxiv.org/abs/1505.02386), [doi:10.1103/PhysRevD.90.104020](https://doi.org/10.1103/PhysRevD.90.104020).
- [25] Robie A. Hennigar, Wilson G. Brenna, and Robert B. Mann. $P-v$ criticality in quasitopological gravity. *JHEP*, 07:077, 2015. [arXiv:1505.05517](https://arxiv.org/abs/1505.05517), [doi:10.1007/JHEP07\(2015\)077](https://doi.org/10.1007/JHEP07(2015)077).
- [26] Elena Caceres, Phuc H. Nguyen, and Juan F. Pedraza. Holographic entanglement entropy and the extended phase structure of STU black holes. *JHEP*, 09:184, 2015. [arXiv:1507.06069](https://arxiv.org/abs/1507.06069), [doi:10.1007/JHEP09\(2015\)184](https://doi.org/10.1007/JHEP09(2015)184).
- [27] Shao-Wen Wei and Yu-Xiao Liu. Insight into the Microscopic Structure of an AdS Black Hole from a Thermodynamical Phase Transition. *Phys. Rev. Lett.*, 115(11):111302, 2015. [Erratum: *Phys.Rev.Lett.* 116, 169903 (2016)]. [arXiv:1502.00386](https://arxiv.org/abs/1502.00386), [doi:10.1103/PhysRevLett.115.111302](https://doi.org/10.1103/PhysRevLett.115.111302).
- [28] Seyed Hossein Hendi, Gu-Qiang Li, Jie-Xiong Mo, Shahram Panahiyan, and Behzad Eslam Panah. New perspective for black hole thermodynamics in Gauss-Bonnet-Born-Infeld massive gravity. *Eur. Phys. J. C*, 76(10):571, 2016. [arXiv:1608.03148](https://arxiv.org/abs/1608.03148), [doi:10.1140/epjc/s10052-016-4410-4](https://doi.org/10.1140/epjc/s10052-016-4410-4).
- [29] S.H. Hendi, R.B. Mann, S. Panahiyan, and B. Eslam Panah. Van der Waals like behavior of topological AdS black holes in massive gravity. *Phys. Rev. D*, 95(2):021501, 2017. [arXiv:1702.00432](https://arxiv.org/abs/1702.00432), [doi:10.1103/PhysRevD.95.021501](https://doi.org/10.1103/PhysRevD.95.021501).
- [30] José P.S. Lemos and Oleg B. Zaslavskii. Black hole thermodynamics with the cosmological constant as independent variable: Bridge between the enthalpy and the Euclidean path integral approaches. *Phys. Lett. B*, 786:296–299, 2018. [arXiv:1806.07910](https://arxiv.org/abs/1806.07910), [doi:10.1016/j.physletb.2018.08.075](https://doi.org/10.1016/j.physletb.2018.08.075).
- [31] Juan F. Pedraza, Watse Sybesma, and Manus R. Visser. Hyperscaling violating black holes with spherical and hyperbolic horizons. *Class. Quant. Grav.*, 36(5):054002, 2019. [arXiv:1807.09770](https://arxiv.org/abs/1807.09770), [doi:10.1088/1361-6382/ab0094](https://doi.org/10.1088/1361-6382/ab0094).
- [32] Peng Wang, Houwen Wu, and Haitang Yang. Thermodynamics and Phase Transitions of Nonlinear Electrodynamics Black Holes in an Extended Phase Space. *JCAP*, 04(04):052, 2019. [arXiv:1808.04506](https://arxiv.org/abs/1808.04506), [doi:10.1088/1475-7516/2019/04/052](https://doi.org/10.1088/1475-7516/2019/04/052).
- [33] Shao-Wen Wei, Yu-Xiao Liu, and Robert B. Mann. Repulsive Interactions and Universal Properties of Charged Anti-de Sitter Black Hole Microstructures. *Phys. Rev. Lett.*, 123(7):071103, 2019. [arXiv:1906.10840](https://arxiv.org/abs/1906.10840), [doi:10.1103/PhysRevLett.123.071103](https://doi.org/10.1103/PhysRevLett.123.071103).
- [34] Shao-Wen Wei and Yu-Xiao Liu. Extended thermodynamics and microstructures of four-dimensional charged Gauss-Bonnet black hole in AdS space. *Phys. Rev. D*, 101(10):104018, 2020. [arXiv:2003.14275](https://arxiv.org/abs/2003.14275), [doi:10.1103/PhysRevD.101.104018](https://doi.org/10.1103/PhysRevD.101.104018).
- [35] Guangzhou Guo, Peng Wang, Houwen Wu, and Haitang Yang. Thermodynamics and Phase Structure of an Einstein-Maxwell-scalar Model in Extended Phase Space. 7 2021. [arXiv:2107.04467](https://arxiv.org/abs/2107.04467).
- [36] Jr. York, James W. Black hole thermodynamics and the Euclidean Einstein action. *Phys. Rev. D*, 33:2092–2099, Apr 1986. URL: <https://link.aps.org/doi/10.1103/PhysRevD.33.2092>, [doi:10.1103/PhysRevD.33.2092](https://doi.org/10.1103/PhysRevD.33.2092).
- [37] Harry W. Braden, J. David Brown, Bernard F. Whiting, and James W. York. Charged black hole in a grand canonical ensemble. *Phys. Rev. D*, 42:3376–3385, Nov 1990. URL: <https://link.aps.org/doi/10.1103/PhysRevD.42.3376>, [doi:10.1103/PhysRevD.42.3376](https://doi.org/10.1103/PhysRevD.42.3376).
- [38] Steven Carlip and S. Vaidya. Phase transitions and critical behavior for charged black holes. *Class. Quant. Grav.*, 20:3827–3838, 2003. [arXiv:gr-qc/0306054](https://arxiv.org/abs/gr-qc/0306054), [doi:10.1088/0264-9381/20/16/319](https://doi.org/10.1088/0264-9381/20/16/319).
- [39] Andrew P. Lundgren. Charged black hole in a canonical ensemble. *Phys. Rev. D*, 77:044014, 2008. [arXiv:gr-qc/0612119](https://arxiv.org/abs/gr-qc/0612119), [doi:10.1103/PhysRevD.77.044014](https://doi.org/10.1103/PhysRevD.77.044014).
- [40] J.X. Lu, Shibaji Roy, and Zhiguang Xiao. Phase transitions and critical behavior of black branes in canonical ensemble. *JHEP*, 01:133, 2011. [arXiv:1010.2068](https://arxiv.org/abs/1010.2068), [doi:10.1007/JHEP01\(2011\)133](https://doi.org/10.1007/JHEP01(2011)133).

- [41] Chao Wu, Zhiguang Xiao, and Jianfei Xu. Bubbles and Black Branes in Grand Canonical Ensemble. *Phys. Rev. D*, 85:044009, 2012. [arXiv:1108.1347](#), [doi:10.1103/PhysRevD.85.044009](#).
- [42] J.X. Lu, Ran Wei, and Jianfei Xu. The phase structure of black D1/D5 (F/NS5) system in canonical ensemble. *JHEP*, 12:012, 2012. [arXiv:1210.0708](#), [doi:10.1007/JHEP12\(2012\)012](#).
- [43] J.X. Lu and Ran Wei. Modulating the phase structure of black D6 branes in canonical ensemble. *JHEP*, 04:100, 2013. [arXiv:1301.1780](#), [doi:10.1007/JHEP04\(2013\)100](#).
- [44] Da Zhou and Zhiguang Xiao. Phase structures of the black Dp-D(p + 4)-brane system in various ensembles I: thermal stability. *JHEP*, 07:134, 2015. [arXiv:1502.00261](#), [doi:10.1007/JHEP07\(2015\)134](#).
- [45] Zhiguang Xiao and Da Zhou. Phase structures of the black Dp-D(p + 4)-brane system in various ensembles II: electrical and thermodynamic stability. *JHEP*, 09:028, 2015. [arXiv:1507.02088](#), [doi:10.1007/JHEP09\(2015\)028](#).
- [46] Nicolas Sanchis-Gual, Juan Carlos Degollado, Pedro J. Montero, José A. Font, and Carlos Herdeiro. Explosion and Final State of an Unstable Reissner-Nordström Black Hole. *Phys. Rev. Lett.*, 116(14):141101, 2016. [arXiv:1512.05358](#), [doi:10.1103/PhysRevLett.116.141101](#).
- [47] Nicolas Sanchis-Gual, Juan Carlos Degollado, Carlos Herdeiro, José A. Font, and Pedro J. Montero. Dynamical formation of a Reissner-Nordström black hole with scalar hair in a cavity. *Phys. Rev. D*, 94(4):044061, 2016. [arXiv:1607.06304](#), [doi:10.1103/PhysRevD.94.044061](#).
- [48] Pallab Basu, Chethan Krishnan, and P. N. Bala Subramanian. Hairy Black Holes in a Box. *JHEP*, 11:041, 2016. [arXiv:1609.01208](#), [doi:10.1007/JHEP11\(2016\)041](#).
- [49] Yan Peng, Bin Wang, and Yunqi Liu. On the thermodynamics of the black hole and hairy black hole transitions in the asymptotically flat spacetime with a box. *Eur. Phys. J. C*, 78(3):176, 2018. [arXiv:1708.01411](#), [doi:10.1140/epjc/s10052-018-5652-0](#).
- [50] Yan Peng. Studies of a general flat space/boson star transition model in a box through a language similar to holographic superconductors. *JHEP*, 07:042, 2017. [arXiv:1705.08694](#), [doi:10.1007/JHEP07\(2017\)042](#).
- [51] Yan Peng. Scalar field configurations supported by charged compact reflecting stars in a curved spacetime. *Phys. Lett. B*, 780:144–148, 2018. [arXiv:1801.02495](#), [doi:10.1016/j.physletb.2018.02.068](#).
- [52] Peng Wang, Haitang Yang, and Shuxuan Ying. Thermodynamics and phase transition of a Gauss-Bonnet black hole in a cavity. *Phys. Rev. D*, 101(6):064045, 2020. [arXiv:1909.01275](#), [doi:10.1103/PhysRevD.101.064045](#).
- [53] Peng Wang, Houwen Wu, and Haitang Yang. Thermodynamics and Phase Transition of a Nonlinear Electrodynamics Black Hole in a Cavity. *JHEP*, 07:002, 2019. [arXiv:1901.06216](#), [doi:10.1007/JHEP07\(2019\)002](#).
- [54] Kangkai Liang, Peng Wang, Houwen Wu, and Mingtao Yang. Phase structures and transitions of Born–Infeld black holes in a grand canonical ensemble. *Eur. Phys. J. C*, 80(3):187, 2020. [arXiv:1907.00799](#), [doi:10.1140/epjc/s10052-020-7750-z](#).
- [55] Peng Wang, Houwen Wu, and Shuxuan Ying. Validity of Thermodynamic Laws and Weak Cosmic Censorship for AdS Black Holes and Black Holes in a Cavity. *Chin. Phys. C*, 45(5):055105, 2021. [arXiv:2002.12233](#), [doi:10.1088/1674-1137/abe5e](#).
- [56] Peng Wang, Houwen Wu, and Haitang Yang. Thermodynamic Geometry of AdS Black Holes and Black Holes in a Cavity. *Eur. Phys. J. C*, 80(3):216, 2020. [arXiv:1910.07874](#), [doi:10.1140/epjc/s10052-020-7776-2](#).
- [57] Fil Simovic and Robert B. Mann. Critical Phenomena of Charged de Sitter Black Holes in Cavities. *Class. Quant. Grav.*, 36(1):014002, 2019. [arXiv:1807.11875](#), [doi:10.1088/1361-6382/aaf445](#).
- [58] Fil Simovic and Robert B. Mann. Critical Phenomena of Born-Infeld-de Sitter Black Holes in Cavities. *JHEP*, 05:136, 2019. [arXiv:1904.04871](#), [doi:10.1007/JHEP05\(2019\)136](#).
- [59] Sumarna Haroon, Robie A. Hennigar, Robert B. Mann, and Fil Simovic. Thermodynamics of Gauss-Bonnet-de Sitter Black Holes. *Phys. Rev. D*, 101:084051, 2020. [arXiv:2002.01567](#), [doi:10.1103/PhysRevD.101.084051](#).
- [60] Peng Wang, Houwen Wu, Haitang Yang, and Feiyu Yao. Extended Phase Space Thermodynamics for Black Holes in a Cavity. *JHEP*, 09:154, 2020. [arXiv:2006.14349](#), [doi:10.1007/JHEP09\(2020\)154](#).
- [61] F. Weinhold. Metric geometry of equilibrium thermodynamics. *The Journal of Chemical Physics*, 63(6):2479–2483, 1975. URL: <https://doi.org/10.1063/1.431689>, [arXiv:https://doi.org/10.1063/1.431689](#), [doi:10.1063/1.431689](#).
- [62] George Ruppeiner. Riemannian geometry in thermodynamic fluctuation theory. *Rev. Mod. Phys.*, 67:605–659, Jul 1995. [Erratum: *Rev.Mod.Phys.* 68, 313–313 (1996)]. URL: <https://link.aps.org/doi/10.1103/RevModPhys.67.605>, [doi:10.1103/RevModPhys.67.605](#).
- [63] Sergio Ferrara, Gary W. Gibbons, and Renata Kallosh. Black holes and critical points in moduli space. *Nucl. Phys. B*, 500:75–93, 1997. [arXiv:hep-th/9702103](#), [doi:10.1016/S0550-3213\(97\)00324-6](#).
- [64] Jan E. Aman, Ingemar Bengtsson, and Narit Pidokrajt. Geometry of black hole thermodynamics. *Gen. Rel. Grav.*, 35:1733, 2003. [arXiv:gr-qc/0304015](#), [doi:10.1023/A:1026058111582](#).
- [65] Tapobrata Sarkar, Gautam Sengupta, and Bhupendra Nath Tiwari. On the thermodynamic geometry of BTZ black holes. *JHEP*, 11:015, 2006. [arXiv:hep-th/0606084](#), [doi:10.1088/1126-6708/2006/11/015](#).
- [66] Hernando Quevedo and Alberto Sanchez. Geometrothermodynamics of asymptotically de Sitter black holes. *JHEP*, 09:034, 2008. [arXiv:0805.3003](#), [doi:10.1088/1126-6708/2008/09/034](#).
- [67] Rabin Banerjee, Sujoy Kumar Modak, and Saurav Samanta. Second Order Phase Transition and Thermodynamic Geometry in Kerr-AdS Black Hole. *Phys. Rev. D*, 84:064024, 2011. [arXiv:1005.4832](#), [doi:10.1103/PhysRevD.84.064024](#).
- [68] Dumitru Astefanesei, Maria J. Rodriguez, and Stefan Theisen. Thermodynamic instability of doubly spinning black objects. *JHEP*, 08:046, 2010. [arXiv:1003.2421](#), [doi:10.1007/JHEP08\(2010\)046](#).
- [69] Haishan Liu, H. Lu, Mingxing Luo, and Kai-Nan Shao. Thermodynamical Metrics and Black Hole Phase Transitions. *JHEP*, 12:054, 2010. [arXiv:1008.4482](#), [doi:10.1007/JHEP12\(2010\)054](#).
- [70] Rabin Banerjee, Bibhas Ranjan Majhi, and Saurav Samanta. Thermogeometric phase transition in a unified framework.

- Phys. Lett. B*, 767:25–28, 2017. [arXiv:1611.06701](#), [doi:10.1016/j.physletb.2017.01.040](#).
- [71] Tsvetan Vetsov. Information Geometry on the Space of Equilibrium States of Black Holes in Higher Derivative Theories. *Eur. Phys. J. C*, 79(1):71, 2019. [arXiv:1806.05011](#), [doi:10.1140/epjc/s10052-019-6553-6](#).
 - [72] H. Dimov, R.C. Rashkov, and T. Vetsov. Thermodynamic information geometry and complexity growth of a warped AdS black hole and the warped AdS₃/CFT₂ correspondence. *Phys. Rev. D*, 99(12):126007, 2019. [arXiv:1902.02433](#), [doi:10.1103/PhysRevD.99.126007](#).
 - [73] Seyed Ali Hosseini Mansoori and Behrouz Mirza. Geometrothermodynamics as a singular conformal thermodynamic geometry. *Phys. Lett. B*, 799:135040, 2019. [arXiv:1905.01733](#), [doi:10.1016/j.physletb.2019.135040](#).
 - [74] Krishnakanta Bhattacharya, Sumit Dey, Bibhas Ranjan Majhi, and Saurav Samanta. General framework to study the extremal phase transition of black holes. *Phys. Rev. D*, 99(12):124047, 2019. [arXiv:1903.03434](#), [doi:10.1103/PhysRevD.99.124047](#).
 - [75] Jian-yong Shen, Rong-Gen Cai, Bin Wang, and Ru-Keng Su. Thermodynamic geometry and critical behavior of black holes. *Int. J. Mod. Phys. A*, 22:11–27, 2007. [arXiv:gr-qc/0512035](#), [doi:10.1142/S0217751X07034064](#).
 - [76] Anurag Sahay, Tapobrata Sarkar, and Gautam Sengupta. On the Thermodynamic Geometry and Critical Phenomena of AdS Black Holes. *JHEP*, 07:082, 2010. [arXiv:1004.1625](#), [doi:10.1007/JHEP07\(2010\)082](#).
 - [77] Chao Niu, Yu Tian, and Xiao-Ning Wu. Critical Phenomena and Thermodynamic Geometry of RN-AdS Black Holes. *Phys. Rev. D*, 85:024017, 2012. [arXiv:1104.3066](#), [doi:10.1103/PhysRevD.85.024017](#).
 - [78] Pankaj Chaturvedi, Sayid Mondal, and Gautam Sengupta. Thermodynamic Geometry of Black Holes in the Canonical Ensemble. *Phys. Rev. D*, 98(8):086016, 2018. [arXiv:1705.05002](#), [doi:10.1103/PhysRevD.98.086016](#).
 - [79] Seyed Ali Hosseini Mansoori, Morteza Rafiee, and Shao-Wen Wei. Universal criticality of thermodynamic curvatures for charged AdS black holes. *Phys. Rev. D*, 102(12):124066, 2020. [arXiv:2007.03255](#), [doi:10.1103/PhysRevD.102.124066](#).
 - [80] Jia-Lin Zhang, Rong-Gen Cai, and Hongwei Yu. Phase transition and thermodynamical geometry of Reissner-Nordström-AdS black holes in extended phase space. *Phys. Rev. D*, 91(4):044028, 2015. [arXiv:1502.01428](#), [doi:10.1103/PhysRevD.91.044028](#).
 - [81] S. H. Hendi, A. Sheykhi, S. Panahiyan, and B. Eslam Panah. Phase transition and thermodynamic geometry of Einstein-Maxwell-dilaton black holes. *Phys. Rev. D*, 92(6):064028, 2015. [arXiv:1509.08593](#), [doi:10.1103/PhysRevD.92.064028](#).
 - [82] Anurag Sahay. Restricted thermodynamic fluctuations and the Ruppeiner geometry of black holes. *Phys. Rev. D*, 95(6):064002, 2017. [arXiv:1604.04181](#), [doi:10.1103/PhysRevD.95.064002](#).
 - [83] Amin Dehyadegari, Ahmad Sheykhi, and Afshin Montakhab. Critical behavior and microscopic structure of charged AdS black holes via an alternative phase space. *Phys. Lett. B*, 768:235–240, 2017. [arXiv:1607.05333](#), [doi:10.1016/j.physletb.2017.02.064](#).
 - [84] Yan-Gang Miao and Zhen-Ming Xu. Microscopic structures and thermal stability of black holes conformally coupled to scalar fields in five dimensions. *Nucl. Phys. B*, 942:205–220, 2019. [arXiv:1711.01757](#), [doi:10.1016/j.nuclphysb.2019.03.015](#).
 - [85] Dandan Li, Shanshan Li, Li-Qin Mi, and Zhong-Heng Li. Insight into black hole phase transition from parametric solutions. *Phys. Rev. D*, 96(12):124015, 2017. [doi:10.1103/PhysRevD.96.124015](#).
 - [86] Yun-Zhi Du, Ren Zhao, and Li-Chun Zhang. Microstructure and Continuous Phase Transition of the Gauss-Bonnet AdS Black Hole. 1 2019. [arXiv:1901.07932](#).
 - [87] Xiong-Ying Guo, Huai-Fan Li, Li-Chun Zhang, and Ren Zhao. Microstructure and continuous phase transition of a Reissner-Nordstrom-AdS black hole. *Phys. Rev. D*, 100(6):064036, 2019. [arXiv:1901.04703](#), [doi:10.1103/PhysRevD.100.064036](#).
 - [88] Shao-Wen Wei, Yu-Xiao Liu, and Robert B. Mann. Ruppeiner Geometry, Phase Transitions, and the Microstructure of Charged AdS Black Holes. *Phys. Rev. D*, 100(12):124033, 2019. [arXiv:1909.03887](#), [doi:10.1103/PhysRevD.100.124033](#).
 - [89] Shao-Wen Wei and Yu-Xiao Liu. Intriguing microstructures of five-dimensional neutral Gauss-Bonnet AdS black hole. *Phys. Lett. B*, 803:135287, 2020. [arXiv:1910.04528](#), [doi:10.1016/j.physletb.2020.135287](#).
 - [90] Pavan Kumar Yerra and Chandrasekhar Bhamidipati. Ruppeiner Geometry, Phase Transitions and Microstructures of Black Holes in Massive Gravity. *Int. J. Mod. Phys. A*, 35(22):2050120, 2020. [arXiv:2006.07775](#), [doi:10.1142/S0217751X20501201](#).
 - [91] Pavan Kumar Yerra and Chandrasekhar Bhamidipati. Ruppeiner curvature along a renormalization group flow. *Phys. Lett. B*, 819:136450, 2021. [arXiv:2007.11515](#), [doi:10.1016/j.physletb.2021.136450](#).
 - [92] Pavan Kumar Yerra and Chandrasekhar Bhamidipati. Novel relations in massive gravity at Hawking-Page transition. 7 2021. [arXiv:2107.04504](#).
 - [93] Brian P. Dolan. Pressure and volume in the first law of black hole thermodynamics. *Class. Quant. Grav.*, 28:235017, 2011. [arXiv:1106.6260](#), [doi:10.1088/0264-9381/28/23/235017](#).